Supporting Information

Hollow-Shell Structured Porous $CoSe_2$ Microspheres Encapsulated by MXene Nanosheets for Advanced Lithium Storage

Lin Hong, [1,2] Shunlong Ju, [2] Yunhe Yang,[1] Jiening Zheng,[2] Guanglin Xia,[2] Zhenguo Huang,[3] Xiaoyun Liu*[1] and Xuebin Yu*[2]

[1] Key Laboratory of Specially Functional Polymeric Materials and Related Technology, Ministry of Education, East China University of Science and Technology, Shanghai 200237, China

[2] Department of Materials Science, Fudan University, Shanghai 200433, China

[3] School of Civil & Environmental Engineering, University of Technology Sydney, Ultimo, New South Wales 2007, Australia

E-mail: yuxuebin@fudan.edu.cn; liuxiaoyun@ecust.edu.cn

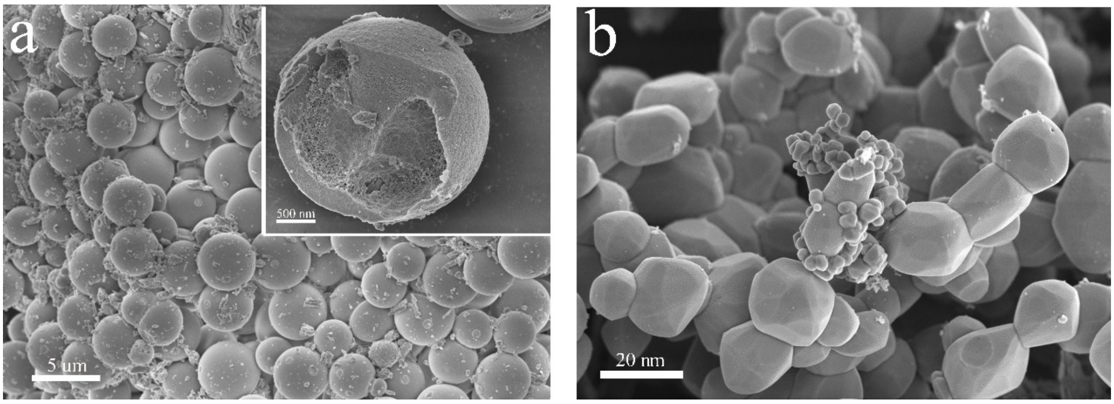

Figure S1 FESEM images of (a) Co-MOF and (b) pure $CoSe_2$.

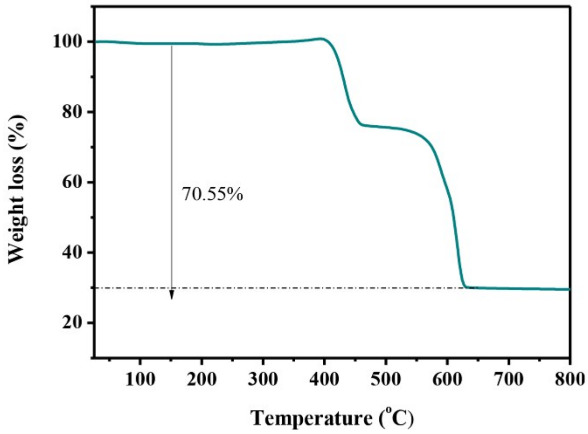

Figure S2 TGA of $CoSe_2$ hollow sphere.

The mass loading of $CoSe_2$ in MOF-derived $CoSe_2$ hollow sphere was determined by TGA in air atmosphere at a heating rate of 10 °C min^{-1} from 25 to 800 °C, as displayed in Figure S3. During the thermal treatment process, the significant mass loss between 400 and 630 °C could be ascribed to the combustion of carbon, and the oxidation of $CoSe_2$ with conversion of Co_3O_4 and Se. When the temperature was further increased, no mass loss could be observed probably owing to the complete transformation of $CoSe_2$ to Co_3O_4. Based on the reaction equation: $3CoSe_2$ (s) + $2O_2$ (g) = Co_3O_4 (s) + 6Se (g) and 70.55 wt.% of the original weight lost, the accurate content of $CoSe_2$ in $CoSe_2$ hollow sphere was calculated to be 79.55 wt.%.

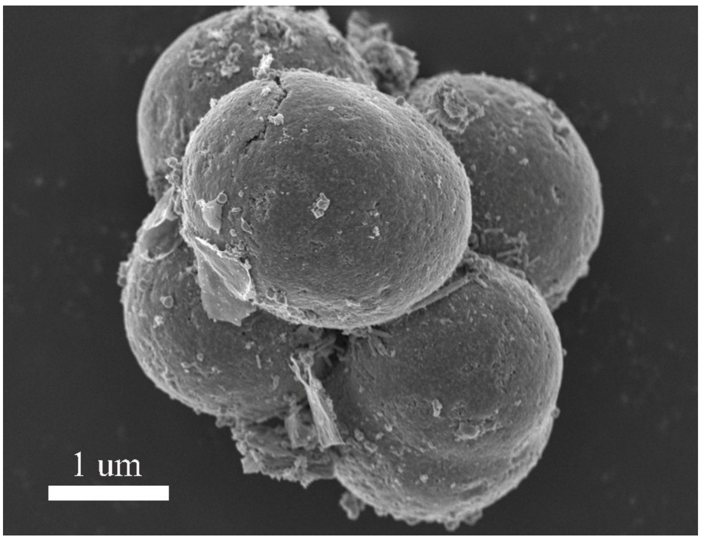

Figure S3 FESEM images of $CoSe_2$@MXene.

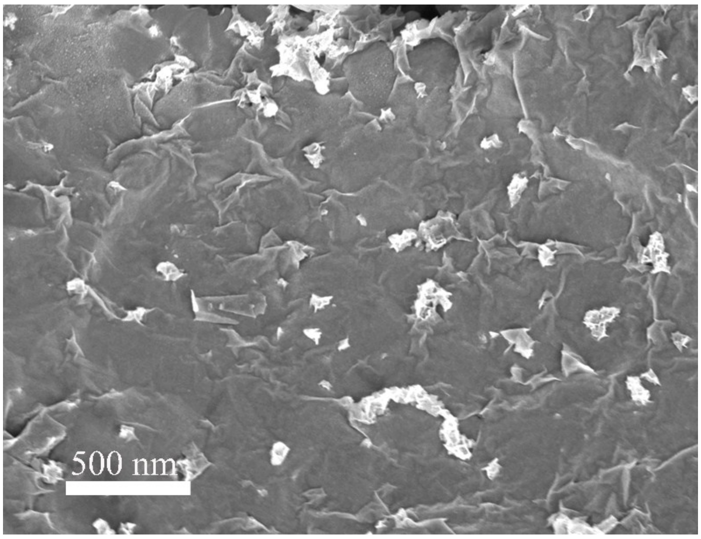

Figure S4 FESEM images of MXene flakes.

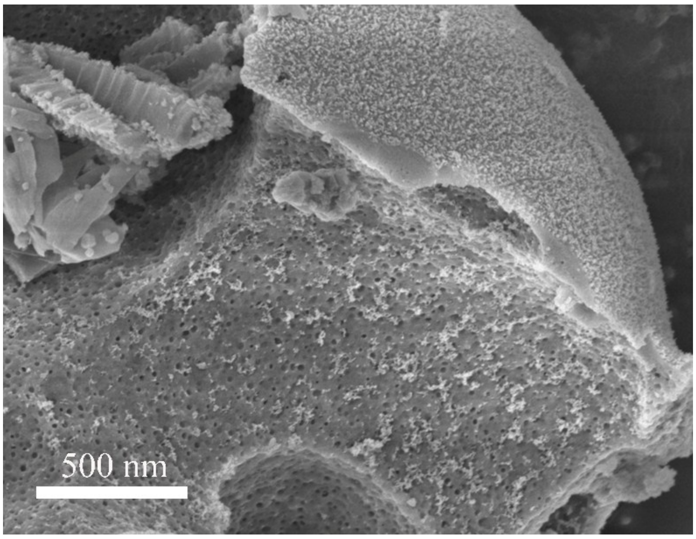

Figure S5 FESEM images of Co-MOF.

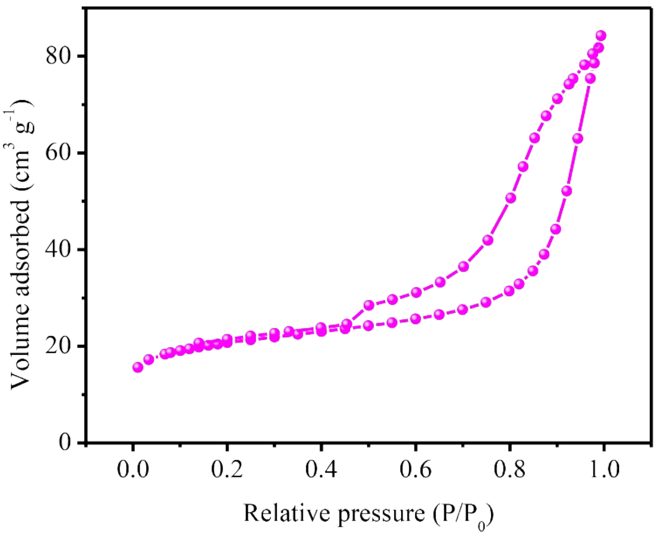

Figure S6 N_2 adsorption-desorption isotherms of $CoSe_2$ spheres.

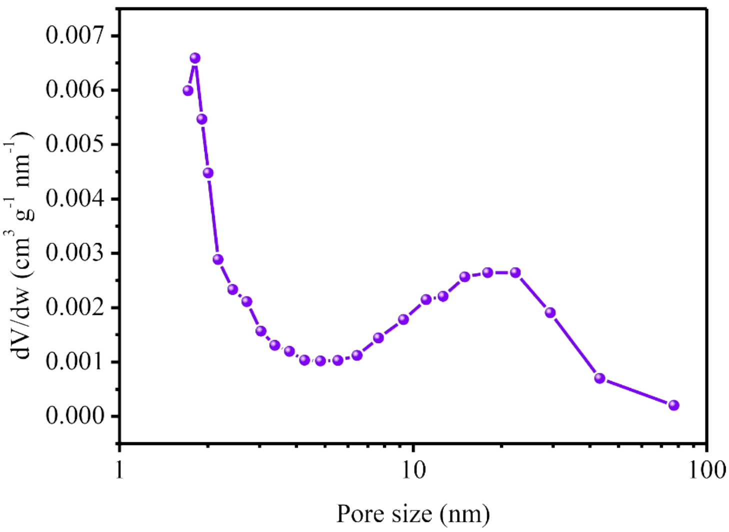

Figure S7 Pore size distribution of $CoSe_2$ spheres.

The $CoSe_2$ spheres possess a specific surface area of 69.19 m^2/g, and a pore volume of 0.116 cm^3/g at $P/P_0 = 0.999$.

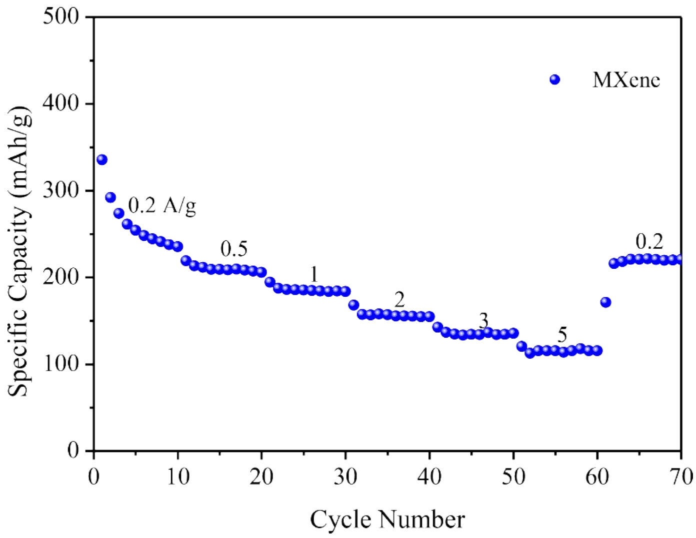

Figure S8 Rate performance of MXene.

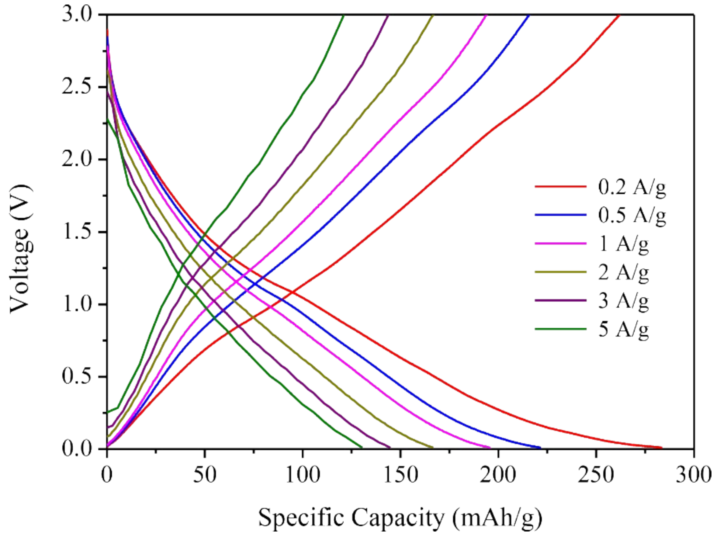

Figure S9 Galvanostatic charge/discharge curves of MXene at various rates.

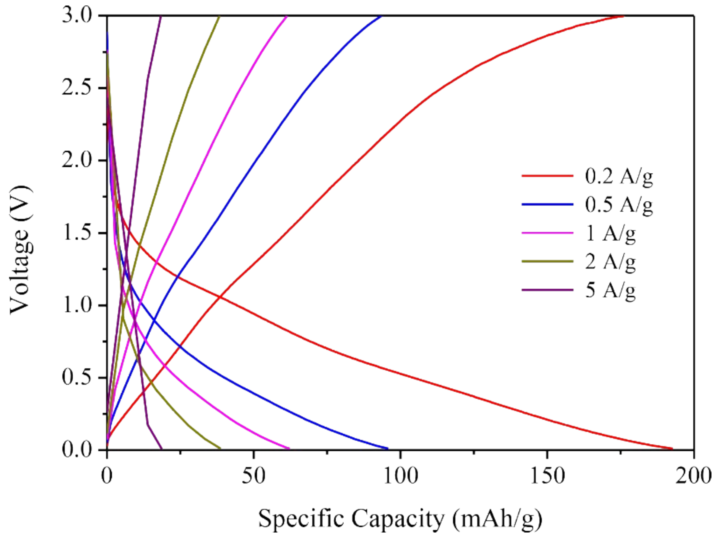

Figure S10 Galvanostatic charge/discharge curves of pure $CoSe_2$ at various rates.

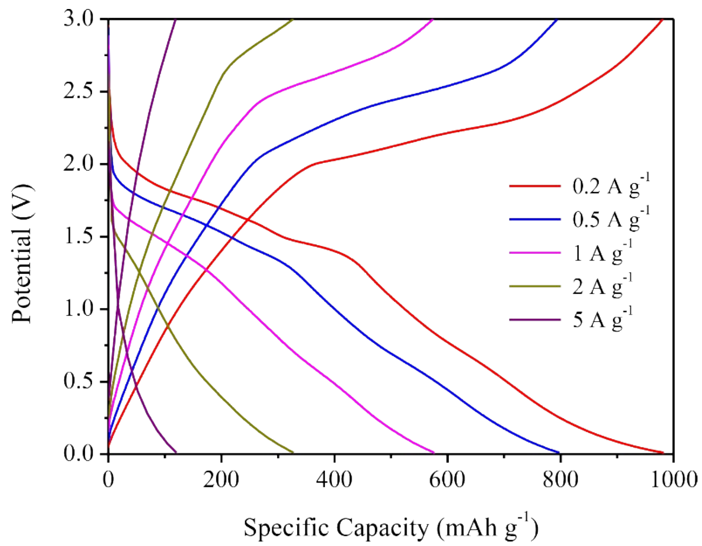

Figure S11 Galvanostatic charge/discharge curves of $CoSe_2$ spheres at various rates.

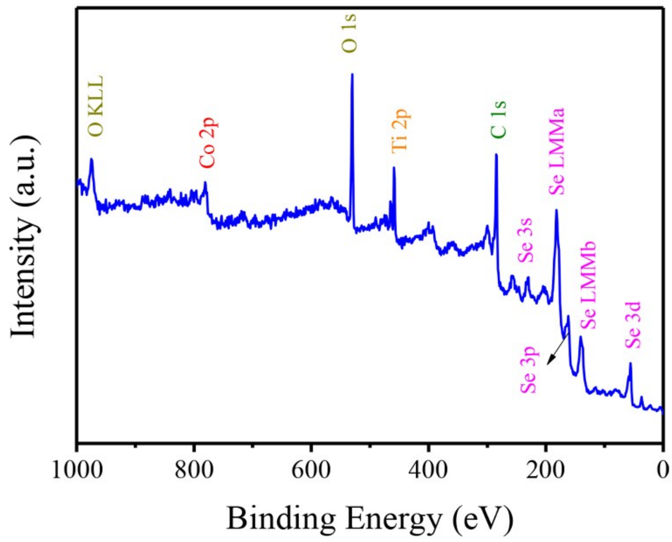

Figure S12 XPS survey spectrum of $CoSe_2$@MXene.

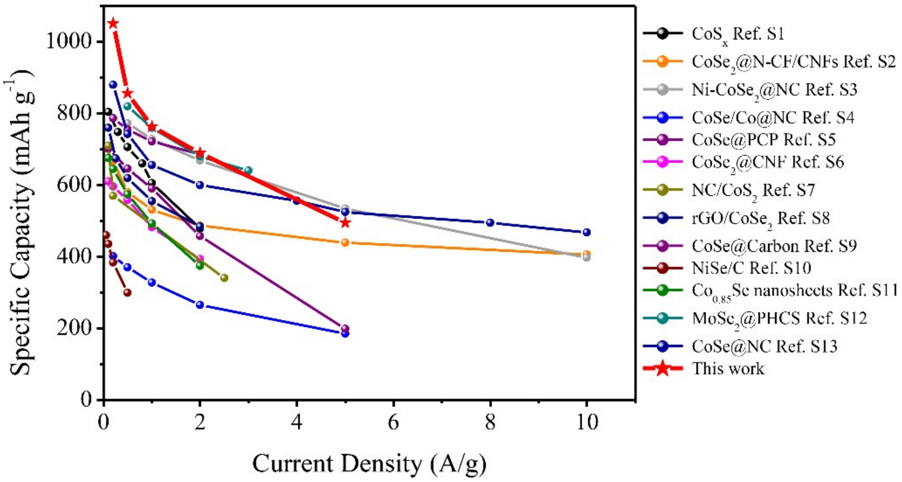

Figure S13 Comparison of rate capability of the produced $CoSe_2$@MXene with other typical anode materials for LIBs.

Table S1 Summary and comparison of cycling and rate performances of recently reported TMDs for LIBs.

Materials	Cycling Performance			Rate Performance		Reference
	Capacity (mAh g^{-1})	Cycles	Current (A g^{-1})	Capacity (mAh g^{-1})	Current (A g^{-1})	
$CoSe_2$@MXene	**910**	**100**	**0.2**	**1051, 856, 763, 669, and 465**	**0.2, 0.5, 1, 2, and 5**	**This work**
CoS_x	1012.1	100	0.5	804, 747, 705, 660, 605, and 478	0.1, 0.3, 0.5, 0.8, 1, and 2	1
$CoSe_2$@N-CF/CNTs	428	500	1	666, 580, 531, 487, 439, and 406	0.2, 0.5, 1, 2, 5, and 10	2
Ni-$CoSe_2$@NC	645	300	1.5	772, 728, 669, 534, and 397	0.5, 1, 2, 5, and 10	3
CoSe/Co@NC	630	100	0.2	401, 370, 328, 265, and 185	0.2, 0.5, 1, 2, and 5	4
CoSe@PCP	675	100	0.2	401, 370, 328, 265, and 185	0.2, 0.5, 1, 2, and 5	5
$CoSe_2$@CNF	1405	300	0.2	610, 596, 559, 482, and 393	0.1, 0.2, 0.5, 1, and 2	6
NC/CoS_2	560	50	0.1	710, 570, 490, and 340	0.1, 0.2, 1, and 2.5	7
rGO/$CoSe_2$	1577	200	0.2	760, 674, 620, 555, and 484	0.1, 0.25, 0.5, 1, and 2	8
CoSe@Carbon	860	100	0.2	787, 755, 722, and 686	0.2, 0.5, 1, and 2	9
NiSe/C	428	50	0.1	460, 435, 384, and 299	0.05, 0.1, 0.2, and 0.5	10
$Co_{0.85}Se$ nanosheets	516	50	0.2	675, 645, 574, 493, and 374	0.1, 0.2, 0.5, 1, and 2	11
$MoSe_2$@PHCs	681	100	0.5	820, 760, 680, and 640	0. 5, 1, 2, and 3	12
CoSe@NC	796	100	1	880, 742, 656, 600, 556, 525, 495, and 374	0.2, 0.5, 1, 2, 4, 5, 8, and 2	13

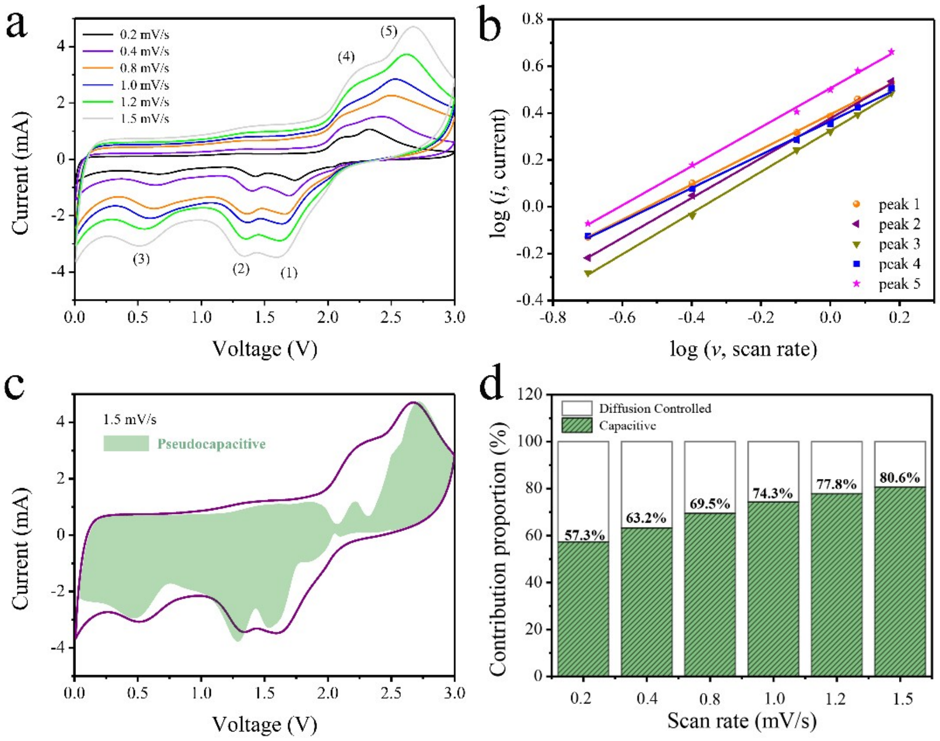

Figure S14 (a) CV profiles of $CoSe_2$@MXene at different scan rates. (b) The plots of log(i) vs log(v) (peak current: i, scan rate: v), calculated from CV curves. (c) The shaded region shows the CV profile with the pseudocapacitive contribution at a scan rate of 1.5 mV s^{-1}. (d) Contribution ratio of pseudocapacitive at different scan rates.

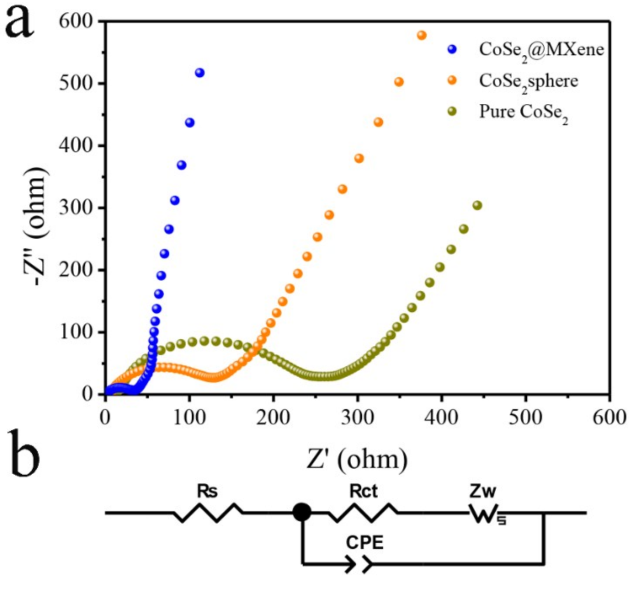

Figure S15 (a) Nyquist plots of pure $CoSe_2$, $CoSe_2$ sphere and $CoSe_2$@MXene electrodes, (b) equivalent circuit model.

References

1. Xiao, Y.; Hwang, J.-Y.; Belharouak, I.; Sun, Y.-K., Superior Li/Na-storage capability of a carbon-free hierarchical CoS_x hollow nanostructure. *Nano Energy* **2017,** 32, 320-328.

2. Yang, J.; Gao, H.; Men, S.; Shi, Z.; Lin, Z.; Kang, X.; Chen, S., $CoSe_2$ Nanoparticles Encapsulated by N-Doped Carbon Framework Intertwined with Carbon Nanotubes: High-Performance Dual-Role Anode Materials for Both Li- and Na-Ion Batteries. *Adv Sci* **2018,** 5, (12), 1800763.

3. Liu, W.; Shao, M.; Zhou, W.; Yuan, B.; Gao, C.; Li, H.; Xu, X.; Chu, H.; Fan, Y.; Zhang, W.; Li, S.; Hui, J.; Fan, D.; Huo, F., Hollow Ni-$CoSe_2$ Embedded in Nitrogen-Doped Carbon Nanocomposites Derived from Metal-Organic Frameworks for High-Rate Anodes. *ACS Appl Mater Interfaces* **2018,** 10, (45), 38845-38852.

4. Zhou, Y.; Tian, R.; Duan, H.; Wang, K.; Guo, Y.; Li, H.; Liu, H., CoSe/Co nanoparticles wrapped by in situ grown N-doped graphitic carbon nanosheets as anode material for advanced lithium ion batteries. *Journal of Power Sources* **2018,** 399, 223-230.

5. Li, J.; Yan, D.; Lu, T.; Yao, Y.; Pan, L., An advanced CoSe embedded within porous carbon polyhedra hybrid for high performance lithium-ion and sodium-ion batteries. *Chemical Engineering Journal* **2017,** 325, 14-24.

6. Wang, J.; Wang, H.; Cao, D.; Lu, X.; Han, X.; Niu, C., Epitaxial Growth of Urchin-Like $CoSe_2$ Nanorods from Electrospun Co-Embedded Porous Carbon Nanofibers and Their Superior Lithium Storage Properties. *Particle & Particle Systems Characterization* **2017,** 34, (10).

7. Wang, Q.; Zou, R.; Xia, W.; Ma, J.; Qiu, B.; Mahmood, A.; Zhao, R.; Yang, Y.; Xia, D.; Xu, Q., Facile Synthesis of Ultrasmall CoS_2 Nanoparticles within Thin N-Doped Porous Carbon Shell for High Performance Lithium-Ion Batteries. *Small* **2015,** 11, (21), 2511-7.

8. Li, Z.; Xue, H.; Wang, J.; Tang, Y.; Lee, C.-S.; Yang, S., Reduced Graphene

Oxide/Marcasite-Type Cobalt Selenide Nanocrystals as an Anode for Lithium-Ion Batteries with Excellent Cyclic Performance. *ChemElectroChem* **2015,** 2, (11), 1682-1686.

9. Hu, H.; Zhang, J.; Guan, B.; Lou, X. W., Unusual Formation of CoSe@carbon Nanoboxes, which have an Inhomogeneous Shell, for Efficient Lithium Storage. *Angew Chem Int Ed Engl* **2016,** 55, (33), 9514-8.

10. Zhang, Z.; Shi, X.; Yang, X., Synthesis of core-shell NiSe/C nanospheres as anodes for lithium and sodium storage. *Electrochimica Acta* **2016,** 208, 238-243.

11. Zhou, J.; Wang, Y.; Zhang, J.; Chen, T.; Song, H.; Yang, H. Y., Two dimensional layered $Co_{0.85}Se$ nanosheets as a high-capacity anode for lithium-ion batteries. *Nanoscale* **2016,** 8, (32), 14992-5000.

12. Yang, X.; Zhang, Z.; Fu, Y.; Li, Q., Porous hollow carbon spheres decorated with molybdenum diselenide nanosheets as anodes for highly reversible lithium and sodium storage. *Nanoscale* **2015,** 7, (22), 10198-203.

13. Liu, J.; Liang, J.; Wang, C.; Ma, J., Electrospun CoSe@N-doped carbon nanofibers with highly capacitive Li storage. *Journal of Energy Chemistry* **2019,** 33, 160-166.